

## Supplementary Material

### The First Porous MOF with Photoswitchable Linker Molecules

Antje Modrow,<sup>a</sup> Dordaneh Zargarani,<sup>b</sup> Rainer Herges,<sup>b</sup> and Norbert Stock<sup>a,\*</sup>

Institut für Anorganische Chemie, Christian-Albrechts-Universität, Max-Eyth-Straße 2,  
D-24118 Kiel (Germany)

Fax: (+49) 0431-880-1775

E-mail: [stock@ac.uni-kiel.de](mailto:stock@ac.uni-kiel.de)

<sup>b</sup>Otto-Diels-Institut für Organische Chemie, Christian-Albrechts-Universität, Otto-  
Hahn-Platz 4, D-24098 Kiel (Germany)

- (1) Synthesis of 3-azo-phenyl-4,4'-bipyridine
- (2) Results of the TG/DTA investigation of CAU-5
- (3) UV/Vis spectrum of CAU-5
- (4) XRPD patterns of the synthesis products obtained from the variation of the molar ratio of 3-azo-phenyl-4,4'-bipyridine : 4,4'-bipyridine
- (5) Raman-spectra of 3-azo-phenyl-4,4'-bipyridine, naphthalenedicarboxylic acid and CAU-5
- (6) CO<sub>2</sub> adsorption isotherm of CAU-5
- (7) Ar adsorption isotherm of CAU-5
- (8) Complete UV/Vis-spectrum of CAU-5 in a BaSO<sub>4</sub> matrix
- (9) Results of the multiple switching experiment of CAU-5
- (10) UV/Vis spectrum of CAU-5, thermal relaxation

### (1) Synthesis of 3-azo-phenyl-4,4'-bipyridine

The synthesis of 3-azo-phenyl-4,4'-bipyridine was accomplished in a 5 step synthesis procedure. All reaction steps, except the last one were carried out according to the literature (references [1] to [4]).

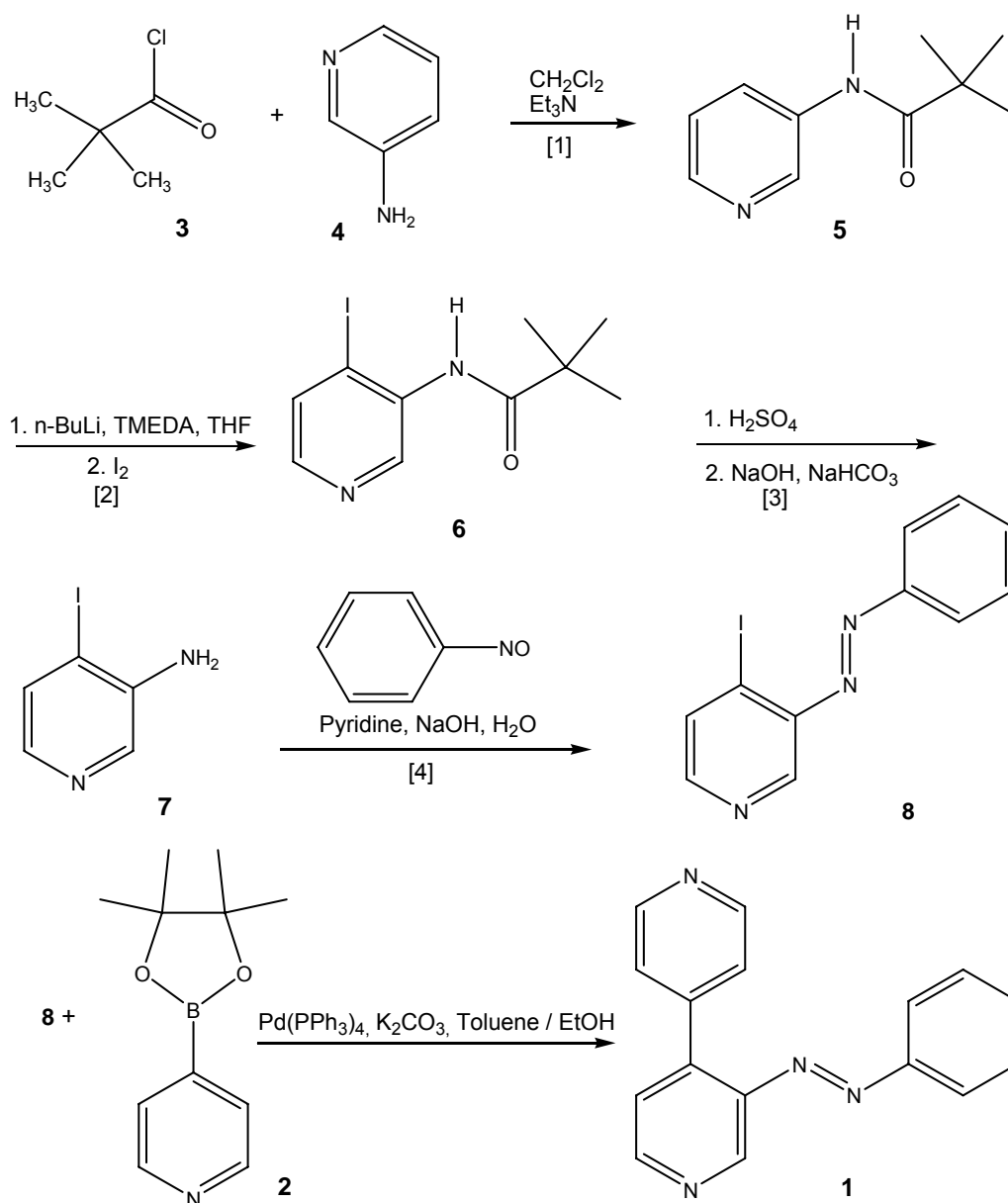


**Figure S1.** Five-step synthesis of the switchable azobipyridine linker molecule (**1**). The first four reaction steps were performed according to the literature.

[1] J. A. Turner, *J. Org. Chem.* **1983**, *48*, 3401.

[2] L. Estel, F. Marsais, G. Quéguiner, *J. Org. Chem.* **1988**, *53*, 2740.

[3] J. Malm, B. Rehn, A.-B. Hörnfeldt, S. Gronowitz, *J. Heterocyclic Chem.* **1994**, *31*, 11.

[4] C. Bornholdt, *Ph. D. Thesis*, Christian-Albrechts-Universität zu Kiel, **2008**.

## (2) Results of the TG/DTA investigation of CAU-5

Figure S2 shows the results of the TG/DTA experiment. A total weight loss of 80.6 % is observed between 390 and 510°C. This is due to the decomposition of the network. The final product was identified as ZnO by PXRD and the calculated weight loss (80.1 %) corresponds well with the measured one.

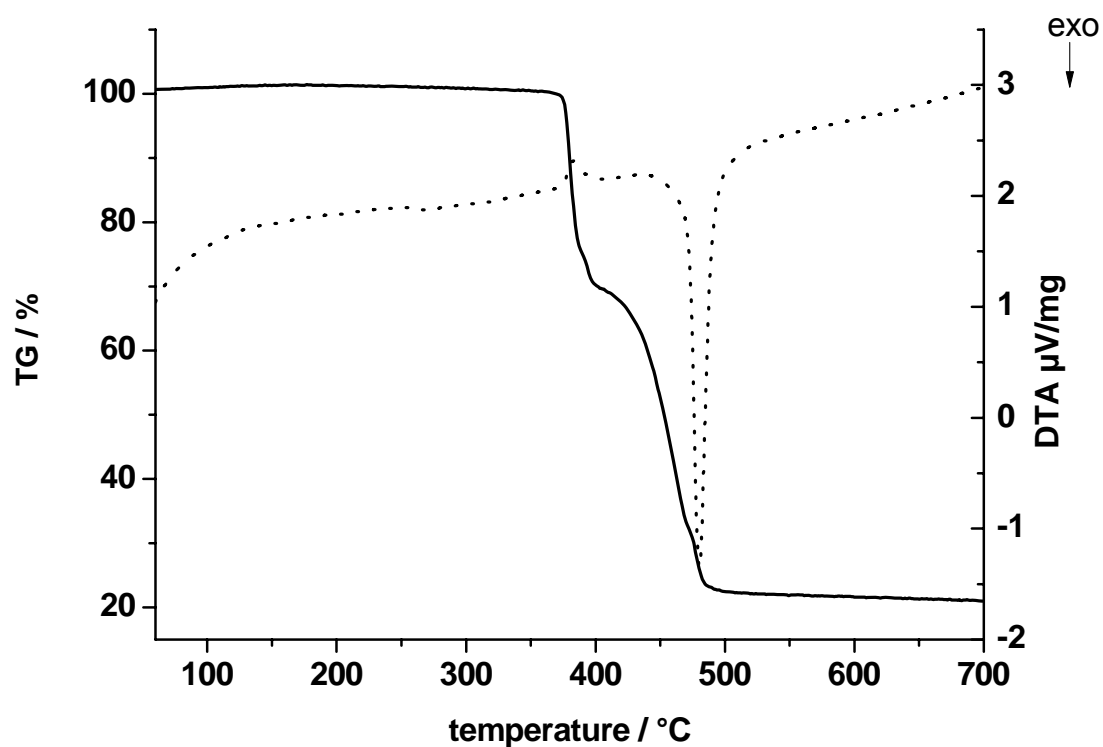


Fig. S2. TG and DTA curve of the thermal decomposition of CAU-5.

### (3) UV/Vis spectrum of CAU-5

Figure S3 shows the results of the UV/Vis switching experiment of CAU-5 microcrystals in a BaSO<sub>4</sub> matrix. After an irradiation period of 5 min with UV light ( $\lambda = 365$  nm) the blue UV/Vis spectrum was recorded. Another 5 min of irradiation with the same wavelength led to the green UV/Vis spectrum. The red UV/Vis spectrum was recorded after an irradiation period of 15 min. This experiment shows, that after an irradiation period of 15 min with UV light ( $\lambda = 365$  nm), the UV/Vis spectrum of CAU-5 in BaSO<sub>4</sub> does not show any further changes. Therefore, 15 min of irradiation was chosen for all switching experiments.

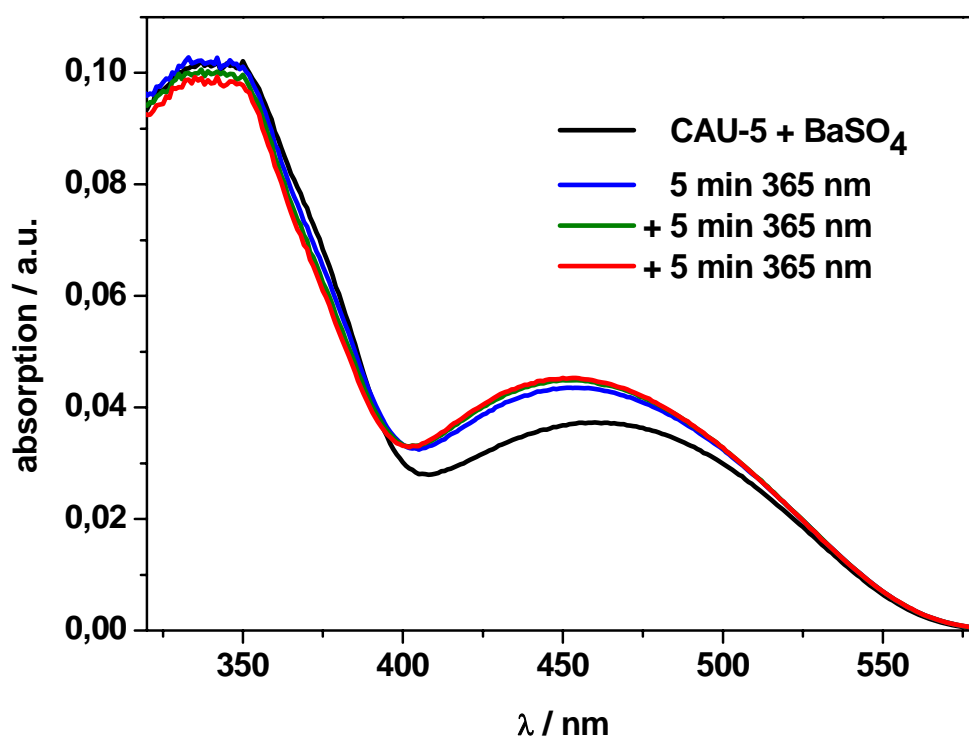


Fig. S3: UV/Vis spectrum of CAU-5 in BaSO<sub>4</sub>: after an irradiation period of 15 min no further change is visible.

**(4) XRPD patterns of the synthesis products obtained from the variation of the molar ratio of 3-azo-phenyl-4,4'-bipyridine : 4,4'-bipyridine**

Figure S4 shows the XRPD patterns of the reaction products from the stepwise replacement of 4,4'-bipyridine by **1**. The comparison of the measurements of the mixed ligand systems with the theoretical powder pattern of  $Zn_2(NDC)_2(4,4'-Bipy)$  (bottom) shows no changes in the reflection positions. The use of pure **1** leads to the new compound CAU-5 (top).

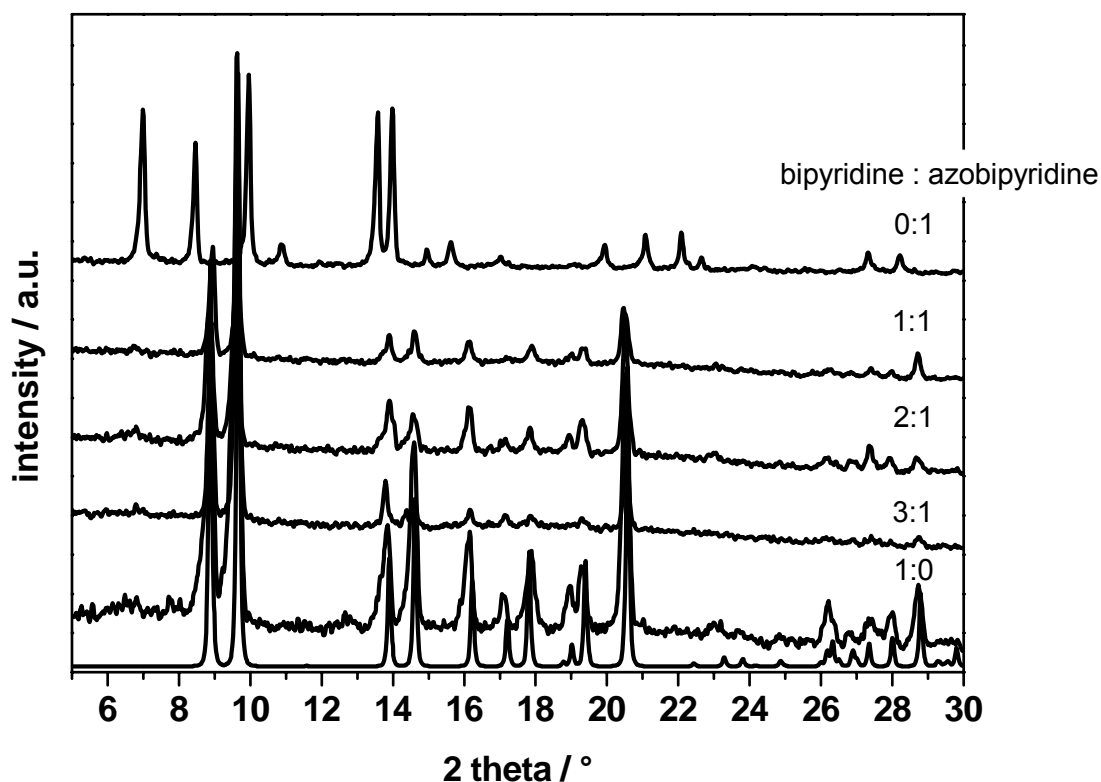


Fig. S4: XRPD pattern of the reaction products obtained by the stepwise replacement of 4,4'-bipyridine by **1**. Bottom: theoretical powder pattern of  $[Zn_2(NDC)_2(4,4'-Bipy)]$ .

### (5) Raman-spectra of 3-azo-phenyl-4,4'-bipyridine, naphthalenedicarboxylic acid and CAU-5

The comparison of the Raman spectra of pure 3-azo-phenyl-4,4'-bipyridine (**1**), H<sub>2</sub>NDC and CAU-5 are shown in Fig. S4. Wavenumbers of the bands are listed in Tab. S1. The characteristic *trans*-N=N- stretching vibration at 1444 cm<sup>-1</sup> (marked by an asterisk) is present in both spectra. Almost all peaks observed in the spectra of H<sub>2</sub>NDC and 3-azo-phenyl-4,4'-bipyridine are also visible in the Raman spectra of CAU-5.

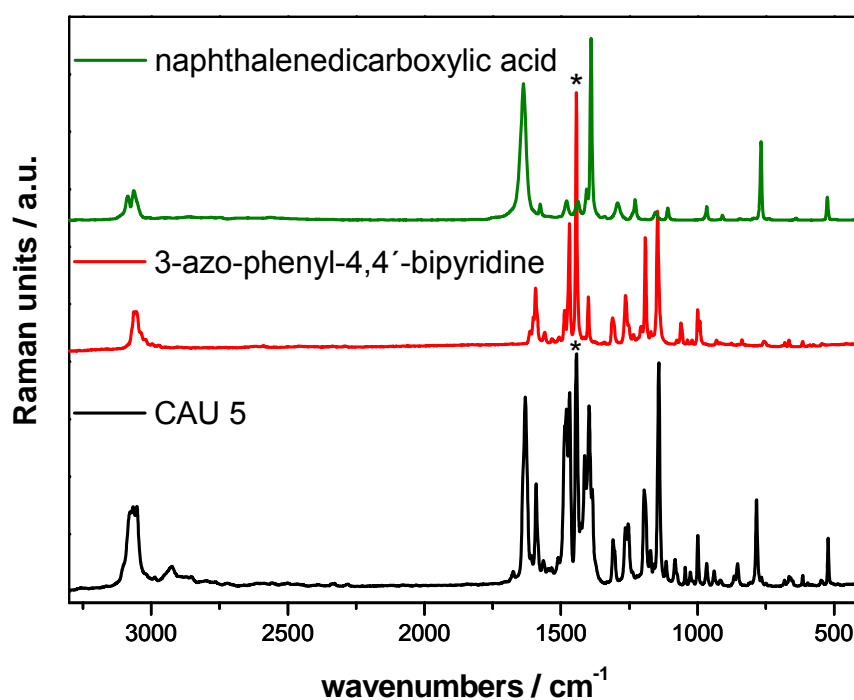


Fig. S5. Raman spectra of naphthalenedicarboxylic acid, 3-azo-phenyl-4,4'-bipyridine and CAU-5.

**Tab. S1: Assignment of Raman-signals.**

<b>1</b>	<b>NDC</b>	<b>CAU 5</b>	<b>assignment</b>
	1636	1631	C=C str. vibration
1594	1577	1591	C=C str. vibration
1485	1479	1481	s-m, C=C, C=N in plane vib. or C-H sym. def. vibr.
1469		1469	s-m, C=C, C=N in plane vib. or C-H sym. def. vibr.
1443		1444	trans N=N vibration
		1427	s-m, C=C, C=N in plane vib.
	1407	1413	s-m, C=C, C=N in plane vib.
1398	1390	1397	aromt. ring vibration
		1385	aromt. ring vibration
1261		1265	arom. C-H in plane def.
1252		1254	arom. C-H in plane def.
1199		1196	arom. C-H in plane def.
		1173	arom. C-H in plane. def. vibr.
1142		1142	arom. C-H in plane def. vibr.
	1109	1115	arom. C-H in plane. def. vibr.
		1083	C=C str. vibr.
		1044	C-O str. vibr. or arom. C-H in plane. def. vibr.
		1025	arom. C-H in plane def. vibr.
998		999	s-m, C=C, C=N in plane vib. or arom. C-H in plane. def. vibr.
	966	966	out-of-plane def. vibr. (3 neigh. H)
		938	out-of-plane def. vibr. (1 isolated H)
		854	Naphthalene rings out-of plane vibr.
	529	522	out of plane def. vibr.

### (6) CO<sub>2</sub> adsorption isotherm of CAU-5

Figure S6 shows the CO<sub>2</sub> adsorption isotherm of CAU-5 at 298 K. The maximum uptake of CO<sub>2</sub> at this temperature and 100 kPa is 50 cm<sup>3</sup>/g.

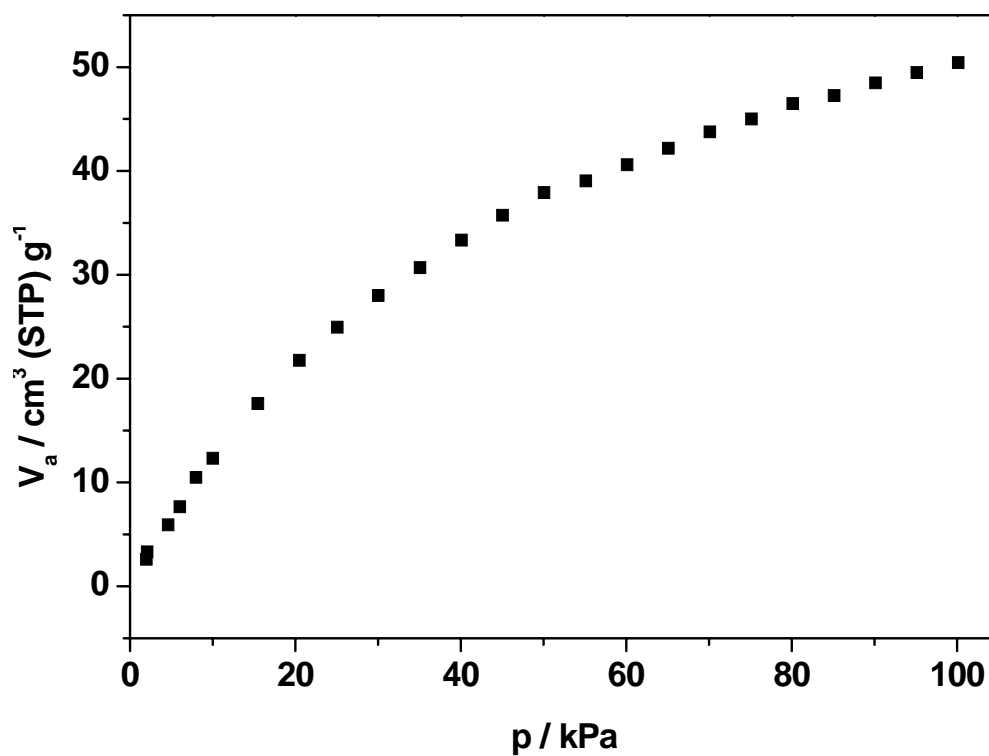


Fig. S6: CO<sub>2</sub> adsorption isotherm of CAU-5 measured at 298 K.



### (7) Ar adsorption isotherm of CAU-5

Figure S7 shows the Ar-adsorption isotherm of CAU-5 at 77 K. Evaluation of the data with the Brunauer-Emmett-Teller (BET) equation results in a specific surface area of 805 m<sup>2</sup>/g.

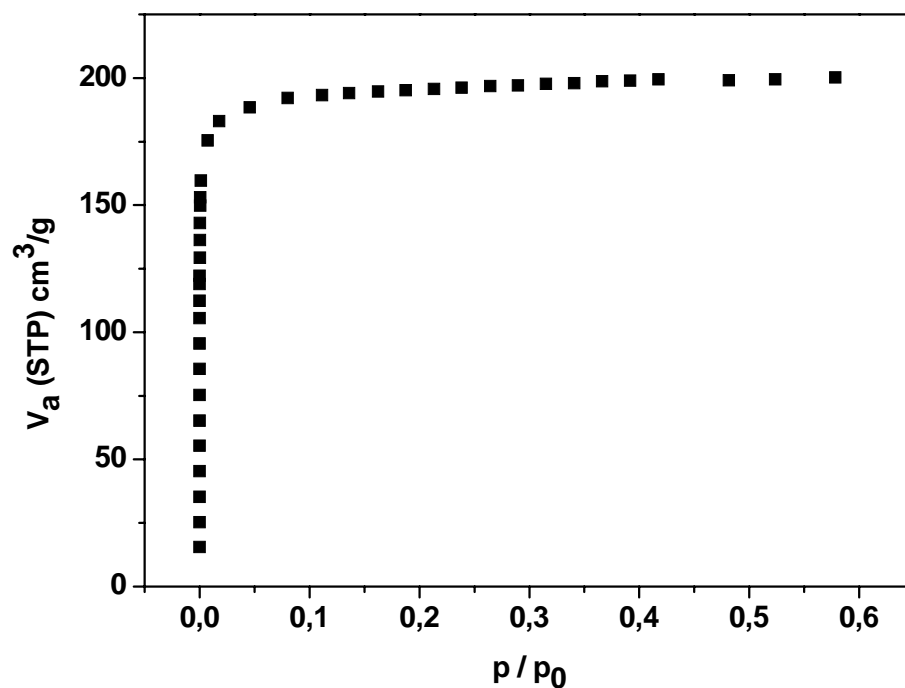


Fig. S7: Ar adsorption isotherm of CAU-5 measured at 77 K.

### (8) Complete UV/Vis-spectrum of CAU-5 in a BaSO<sub>4</sub> matrix

Figure S8 shows the complete UV/Vis Spectrum from 320 to 600 nm of CAU-5 in a BaSO<sub>4</sub> matrix. After an irradiation time of 15 min with UV light ( $\lambda = 365$  nm) (blue, gray, purple curve) the  $\pi \rightarrow \pi^*$  maximum decreased and the  $n \rightarrow \pi^*$  maximum increased due to higher *cis*-isomer concentration. After an irradiation time of 15 min with visible light ( $\lambda = 440$  nm) (orange, red, green curve) the  $\pi \rightarrow \pi^*$  maximum increased again and the  $n \rightarrow \pi^*$  maximum decreased due to lower *cis*-isomer concentration.

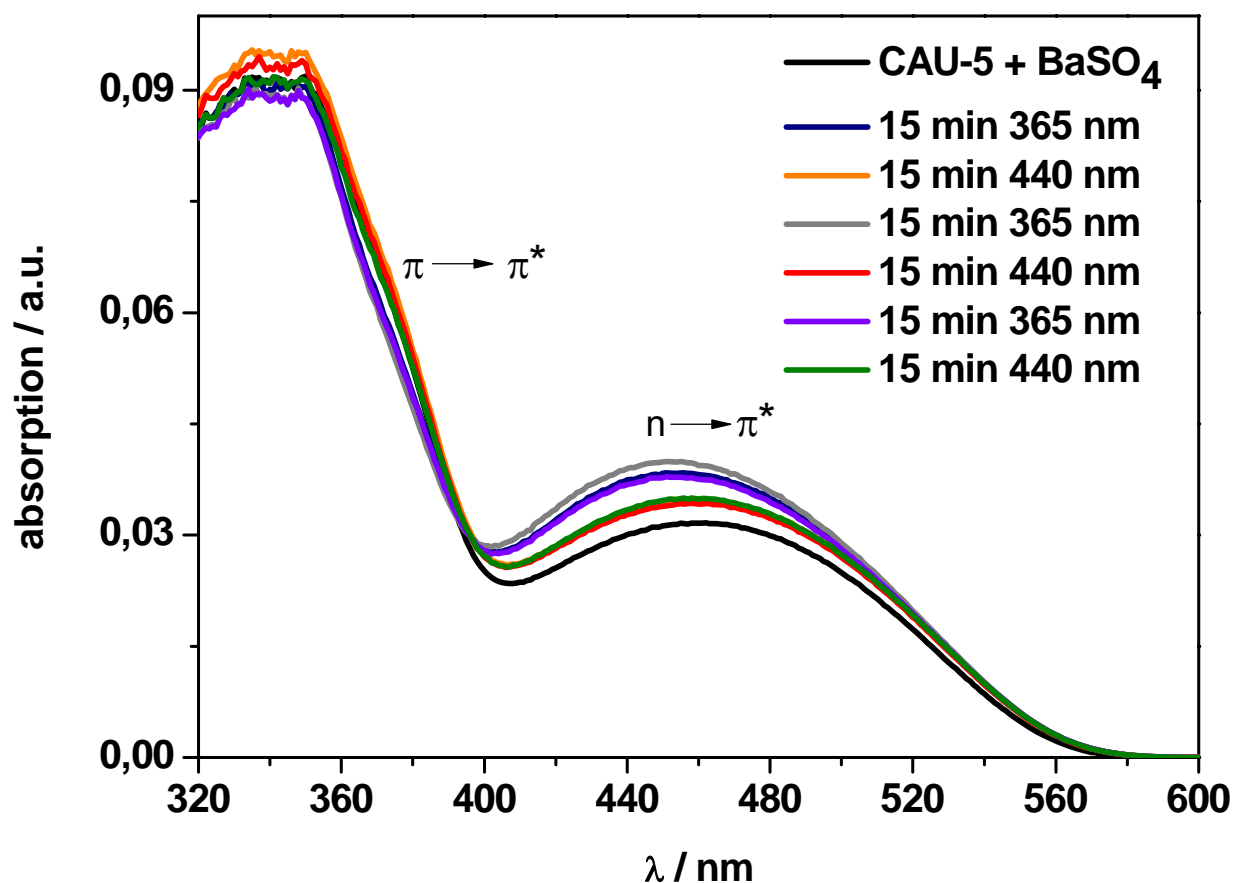


Fig. S8: UV/Vis spectrum of CAU-5: investigation of the switching behavior.

### (9) Results of the multiple switching experiment of CAU-5

Figure S9 shows the absorption intensity at the maximum at 460 nm after the switching cycles (0.5 corresponds to the as synthesized material, cycles 1, 2, and 3 to switching with  $\lambda = 365$  nm, and cycles 1,5, 2.5, and 3.5 to switching with  $\lambda = 440$  nm). For fully reversible switching an ideal zig-zag curve should be observed.

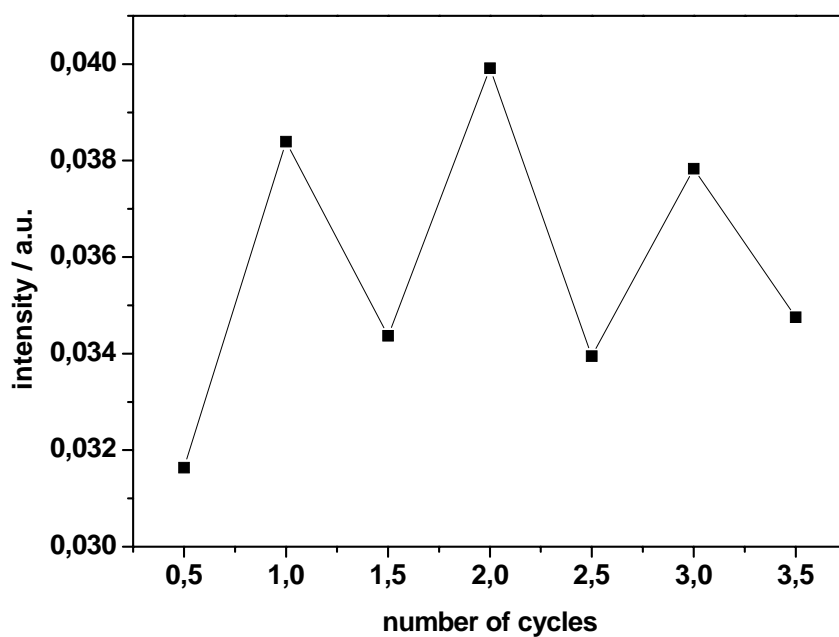


Fig. S9: Switching behavior of CAU-5 in BaSO<sub>4</sub>.

### (10) UV/Vis-spectrum of CAU-5, thermal relaxation

Figure S9 shows the UV/Vis spectra of CAU-5 in a BaSO<sub>4</sub> matrix. After an irradiation time of 15 min with UV light ( $\lambda = 365$  nm) (green curve) the sample was left at room temperature in the dark for 24 h. After 24 h the red UV/Vis spectrum was recorded. The intensity at 460 nm decreased, but did not reach the original value at this point.

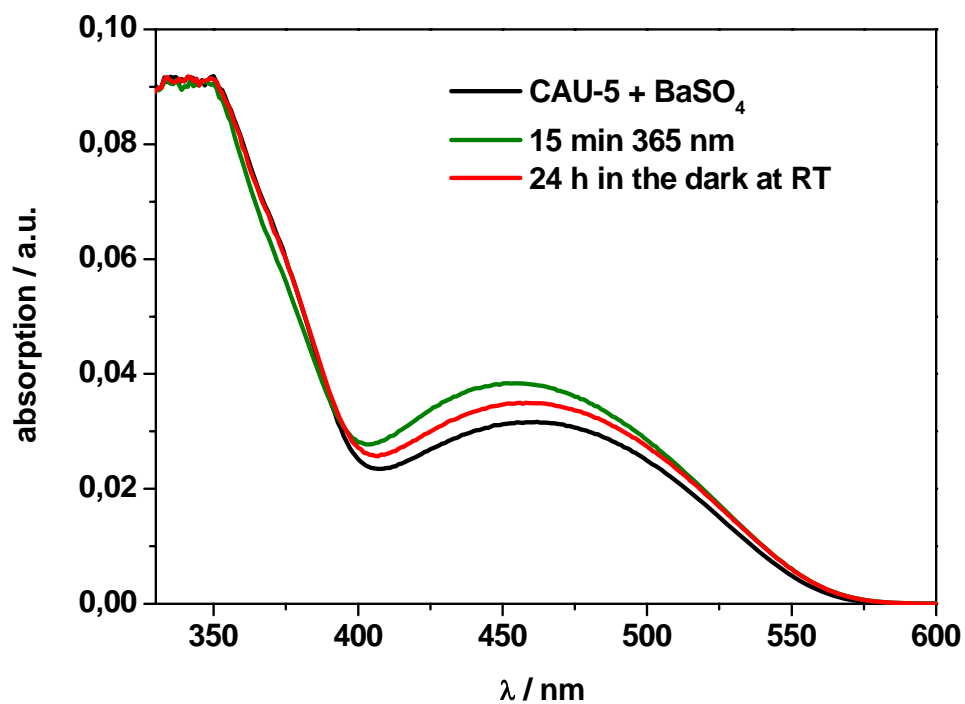


Fig. S10: UV/Vis spectrum of CAU-5: investigation of the thermal relaxation.